# Semiclassical propagation of wavepackets with complex and real trajectories

**M A M de Aguiar**[1]**, M Baranger**[2,3]**, L Jaubert**[4]**, Fernando Parisio**[1]
**and A D Ribeiro**[1]

[1] Instituto de Física 'Gleb Wataghin', Universidade Estadual de Campinas, 13083-970, Campinas, Brazil
[2] Physics Department, University of Arizona, Tucson, AZ 85719, USA
[3] Center for Theoretical Physics, Laboratory for Nuclear Science and Department of Physics, Massachusetts Institute of Technology, Cambridge, MA 02139, USA
[4] Laboratoire de Physique, École Normale Supérieure de Lyon, 46 Allée d'Italie, 69364 Lyon Cedex 07, France

## Abstract

We consider a semiclassical approximation, first derived by Heller and coworkers, for the time evolution of an originally Gaussian wave packet in terms of complex trajectories. We also derive additional approximations replacing the complex trajectories by real ones. These yield three different semiclassical formulae involving different real trajectories. One of these formulae is Heller's thawed Gaussian approximation. The other approximations are non-Gaussian and may involve several trajectories determined by mixed initial–final conditions. These different formulae are tested for the cases of scattering by a hard wall, scattering by an attractive Gaussian potential and bound motion in a quartic oscillator. The formula with complex trajectories gives good results in all cases. The non-Gaussian approximations with real trajectories work well in some cases, whereas the thawed Gaussian works only in very simple situations.

PACS number: 03.65.Sq

## 1. Introduction

The Feynman propagator $\langle x_f | K(T) | x_i \rangle = \langle x_f | \exp(-iHT/\hbar) | x_i \rangle$ can be interpreted as the time evolution of a wavefunction $\psi(x_f, T)$ that is initially localized at $x_i$, $\psi(x, 0) = \delta(x - x_i)$. In the semiclassical limit $\langle x_f | K(T) | x_i \rangle$ can be obtained from the classical trajectories connecting the initial point $x_i$ to the final point $x_f$ in time $T$. The formula which does this is known as the Van Vleck approximation.

One is more likely, however, to be interested in the propagation of a smooth wavepacket, say $\psi_0(x)$, rather than an eigenfunction of the position or momentum operators. The

straightforward way to accomplish this propagation, given knowledge of $K(T)$, is with an extra integration, thus

$$\psi(x_f, T) = \int \langle x_f | K(T) | x_i \rangle \, \mathrm{d}x_i \langle x_i | \psi_0 \rangle. \tag{1.1}$$

In the semiclassical limit this formula becomes

$$\psi_{\mathrm{sc}}(x_f, T) = \int \langle x_f | K(T) | x_i \rangle_{\mathrm{VanVleck}} \, \mathrm{d}x_i \langle x_i | \psi_0 \rangle. \tag{1.2}$$

One problem with this approach is that there are usually several classical trajectories going from $x_i$ to $x_f$ and they are hard to find, the so-called root-search difficulty. We shall return to a discussion of this point in section 7. In this paper, we shall accept the root-search problem and start from equation (1.2).

The main purpose of this paper is to derive various approximations for equation (1.2) and to test them in simple problems. Hence we restrict ourselves here to systems with one degree of freedom. In principle, all the expressions that we obtain are easily generalized to multi-dimensional systems. In practice, of course, the difficulty of the numerical calculations increases very fast with the dimensionality, and it also depends on the actual approximation used.

We shall evaluate the integral by the method of steepest descent which is also often called, somewhat inaccurately, stationary phase. We shall see that the stationary point is generally complex, giving rise to complex classical dynamics. Such a calculation was performed first by Heller and collaborators [Hel87, Hel88]. The result that they derived can be shown to be identical to our equation (2.14). They used it to calculate the motion of a wavepacket in the Morse potential. Their work does not seem to have received from physicists all the recognition that it deserves. Perhaps this was because there were two rather lengthy papers which contained many somewhat unfamiliar notions. Their first paper [Hel87] reached the result through heuristic arguments and the second one [Hel88], though more direct, made many references to the first. In our paper, on the other hand, we shall present in section 2 a very simple and very short derivation of Heller's formula, equation (2.14).

This basic complex approximation will be the starting point for all other developments of this paper. We shall show that it can be handled for relatively simple problems, but we shall also derive three subsequent approximations involving only real trajectories, which are different for each of the three cases. One case yields the well-known Heller thawed Gaussian approximation (TGA) [Hel75]. The other two give different results and we shall show that they can be quite accurate in some situations. We shall illustrate the application of the various semiclassical formulae with two very simple examples (section 4) and two not so simple ones (sections 5 and 6). We hope that our derivation of the basic formula and our examples comparing the several approximations will stimulate new interest in semiclassical formulae derived from complex trajectories.

In order to simplify our calculations we take for initial state $|\psi_0\rangle$ a Gaussian wavefunction with average position and momentum $q$ and $p$ respectively, and position uncertainty $\Delta q = b/\sqrt{2}$. This state is also the coherent state $|z\rangle$ of a harmonic oscillator of mass $\mu$ and frequency $\omega$. It is defined by

$$|z\rangle = \mathrm{e}^{-\frac{1}{2}|z|^2} \, \mathrm{e}^{z\hat{a}^\dagger} |0\rangle \tag{1.3}$$

with $|0\rangle$ the harmonic oscillator ground state and

$$\hat{a}^\dagger = \frac{1}{\sqrt{2}} \left( \frac{\hat{q}}{b} - \mathrm{i}\frac{\hat{p}}{c} \right), \qquad z = \frac{1}{\sqrt{2}} \left( \frac{q}{b} + \mathrm{i}\frac{p}{c} \right). \tag{1.4}$$

In the above $\hat{q}$, $\hat{p}$ and $\hat{a}^\dagger$ are operators; $q$ and $p$ are real numbers; $z$ is complex. The parameters

$$b = (\hbar/\mu\omega)^{\frac{1}{2}} \qquad \text{and} \qquad c = (\hbar\mu\omega)^{\frac{1}{2}} \tag{1.5}$$

define the length and momentum scales, respectively, and their product is $\hbar$. The final form of equation (1.2), our semiclassical approximation for wavepacket propagation, is then

$$\langle x_f|K(T)|z\rangle \approx \int \langle x_f|K(T)|x_i\rangle_{\text{VanVleck}} \, dx_i \langle x_i|z\rangle \equiv \psi_{\text{sc}}(x_f, z; T). \tag{1.6}$$

## 2. Approximation with complex trajectories

Before we perform the integral in equation (1.6) by stationary phase, we recall the relations between the elements of the tangent matrix $m$ and the second derivatives of the action function $S(x_f, x_i; T)$ computed along the real classical trajectory connecting $x_i$ to $x_f$ in time $T$. Given a classical trajectory $X(t)$, $P(t)$ with $X(0) = x_i$ and $X(T) = x_f$, its tangent matrix $m$ connects, in the linearized approximation, a small initial displacement $\delta x_i$, $\delta p_i$ about the trajectory at $t = 0$ to the propagated displacements $\delta x_f$, $\delta p_f$ at time $T$. The relation between $m$ and the second derivatives of the action is

$$\begin{pmatrix} \frac{\delta x_f}{b} \\ \frac{\delta p_f}{c} \end{pmatrix} = \begin{pmatrix} -\frac{S_{ii}}{S_{if}} & -\frac{c}{b}\frac{1}{S_{if}} \\ \frac{b}{c}\left(S_{if} - S_{ff}\frac{S_{ii}}{S_{if}}\right) & -\frac{S_{ff}}{S_{if}} \end{pmatrix} \begin{pmatrix} \frac{\delta x_i}{b} \\ \frac{\delta p_i}{c} \end{pmatrix} \equiv \begin{pmatrix} m_{qq} & m_{qp} \\ m_{pq} & m_{pp} \end{pmatrix} \begin{pmatrix} \frac{\delta x_i}{b} \\ \frac{\delta p_i}{c} \end{pmatrix} \tag{2.1}$$

where $S_{ii} \equiv \partial^2 S/\partial x_i{}^2$, $S_{if} = S_{fi} \equiv \partial^2 S/\partial x_i \partial x_f$ and $S_{ff} \equiv \partial^2 S/\partial x_f{}^2$. A derivation of this formula can be found, for instance, in section (2.6) of [Bar01]. Note that we define $m$ using the coherent state scales $b$ and $c$. Inverting this equation we obtain

$$S_{ii} = \frac{c}{b}\frac{m_{qq}}{m_{qp}}, \qquad S_{if} = -\frac{c}{b}\frac{1}{m_{qp}}, \qquad S_{ff} = \frac{c}{b}\frac{m_{pp}}{m_{qp}}. \tag{2.2}$$

We shall write our final results in terms of elements of the tangent matrix $m$, rather than in terms of derivatives of the action. In this notation the Van Vleck propagator is

$$\langle x_f|K(T)|x_i\rangle_{\text{Van Vleck}} = \frac{1}{b\sqrt{2\pi m_{qp}}} \, e^{iS/\hbar - i\pi/4}. \tag{2.3}$$

For short times $m_{qp}$ is positive and the square root is well defined. For longer times $m_{qp}$ may become negative by going through zero. This happens at the focal points. At these points the Van Vleck formula diverges and must be replaced by a higher order approximation involving Airy functions. Sufficiently away from the focii the approximation becomes good again, as long as one replaces $m_{qp}$ by its modulus and subtracts a phase $\pi/2$ for every focus encountered along the trajectory. We shall not write these so-called Morse phases explicitly because they will cancel out in our final formula.

The overlap $\langle x_i|z\rangle$ is given by

$$\langle x_i|z\rangle = \pi^{-\frac{1}{4}}b^{-\frac{1}{2}} \exp\left(-\frac{(x_i - q)^2}{2b^2}\right) \exp\left(\frac{i}{\hbar} p(x_i - q/2)\right). \tag{2.4}$$

In the semiclassical limit the propagated wavepacket (1.6) is then

$$\psi_{\text{sc}}(x_f, z; T) = \int \frac{\exp\{\Phi\}}{b^{3/2}\pi^{1/4}\sqrt{2\pi m_{qp}}} \, dx_i \tag{2.5}$$

with

$$\Phi(x_f, x_i, T) = \frac{i}{\hbar}[S + p(x_i - q/2)] - \frac{(x_i - q)^2}{2b^2} - i\pi/4. \tag{2.6}$$

We shall now approximate the integration over $x_i$ by the stationary phase method. To do so we assume that the pre-factor in (2.5) is a slowly varying function of $x_i$, which means that the stationary point $x_0$ will be computed by imposing zero variation on $\Phi$ alone. The pre-factor will be simply computed at $x_0$ and will not be expanded. We refer to section 3.3 of [Bar01] for a discussion of this procedure. We need to calculate the first and second derivatives of $\Phi$. The first derivative is

$$\Phi' \equiv \frac{\partial \Phi}{\partial x_i} = \frac{i}{\hbar}(p - p_i) - \frac{(x_i - q)}{b^2} \tag{2.7}$$

where we have defined

$$p_i(x_f, x_i; T) = -\frac{\partial S}{\partial x_i}. \tag{2.8}$$

The second derivative is

$$\Phi'' \equiv \frac{\partial^2 \Phi}{\partial x_i{}^2} = -\frac{i}{\hbar}\frac{\partial p_i}{\partial x_i} - \frac{1}{b^2}. \tag{2.9}$$

The stationary position $x_0(x_f, T)$, solution of the stationary phase condition $\Phi' = 0$, is given by the equation

$$\frac{x_0 - q}{b} + i\frac{p_0 - p}{c} = 0 \tag{2.10}$$

where we have used $c = \hbar/b$ and have made the definition

$$p_0(x_f; T) = p_i(x_f, x_0; T). \tag{2.11}$$

Equation (2.10) makes it clear that $x_0$ is usually complex, and therefore the stationary classical trajectory itself is complex. It leaves $x_0$ at time 0 with momentum $p_0$, also complex, and it arrives at $x_f$, which is real, at time $T$. It goes without saying that, for such a complex trajectory, the tangent matrix $m$ is complex as well.

To integrate over $x_i$, we expand $\Phi$ around $x_0$ to second order, which means that we write $\Phi \approx \Phi(x_0) + \Phi''(x_0)(x_i - x_0)^2/2$. If $\text{Im}(\partial p_i/\partial x_i)$ is less than $\hbar/b^2$ at $x_0$, then $\text{Re}(\Phi)$ has a negative definite quadratic term and the integral can be performed in the Gaussian approximation. Assuming this to be the case we find

$$\psi_{\text{sc}}(x_f, z; T) = \frac{1}{b^{3/2}\pi^{1/4}\sqrt{2\pi m_{qp}}}\sqrt{\frac{-2\pi}{\Phi''(x_0)}}\exp\{\Phi(x_0)\}. \tag{2.12}$$

Finally, using equations (2.9), (2.8), (2.2), we note that

$$\Phi''(x_0) = \frac{i}{\hbar}S_{ii} - \frac{1}{b^2} = \frac{i}{b^2}\frac{m_{qq} + im_{qp}}{m_{qp}}. \tag{2.13}$$

This simplifies the pre-factor in (2.12) and we get

$$\psi_{\text{CT}}(x_f, z; T) = \frac{1}{b^{1/2}\pi^{1/4}}\frac{1}{\sqrt{m_{qq} + im_{qp}}}$$

$$\times \exp\left[\frac{i}{\hbar}S(x_f, x_0; T) + \frac{i}{\hbar}p(x_0 - q/2) - \frac{(x_0 - q)^2}{2b^2}\right]. \tag{2.14}$$

We have changed the subscript on $\psi$ from 'sc' to 'CT' to indicate that this semiclassical approximation is calculated with complex trajectories.

Equation (2.14), the semiclassical limit of the propagated wavepacket, is the Heller result [Hel87, Hel88]. It is the basic result from which all other approximations in this paper are derived. It is *not* an initial value representation and it may involve more than one complex

classical trajectory. At first glance one might think that this formula represents a frozen Gaussian, since the quadratic term in the exponent has a fixed width $b$. A closer look, however, reveals that, since the classical trajectory is complex, all other terms in the exponent also contribute a real part, which changes the effective width: the complex character of the stationary trajectory makes the wavepacket thaw and, at the same time, assume non-Gaussian shapes. Note that no Morse index or phases of $\pi/4$ appear in (2.14). At $T = 0$ one has $m_{qq} = 1, m_{qp} = 0$: one chooses the positive square root and the overlap (2.4) is recovered. For other times one simply follows the phase of the complex number $m_{qq} + \mathrm{i}m_{qp}$ to get the phase of the pre-factor.

Before we close this section we re-write the boundary conditions for the complex trajectories in a more convenient form. The stationary trajectory starts at $x_0$ (usually complex) and ends at $x_f$ (always real). The initial momentum (also complex) is $p_0$, given by (2.11) and (2.8). Since the coordinates $X(t)$ and $P(t)$ along the trajectory are both going to be complex, it is convenient to define the variables

$$u = \frac{1}{\sqrt{2}} \left( \frac{X}{b} + \mathrm{i}\frac{P}{c} \right) \qquad v = \frac{1}{\sqrt{2}} \left( \frac{X}{b} - \mathrm{i}\frac{P}{c} \right) \tag{2.15}$$

where $u \neq v^*$ in general. In this notation Hamilton's equations read

$$\mathrm{i}\hbar\dot{u} = \frac{\partial H}{\partial v} \qquad \text{and} \qquad -\mathrm{i}\hbar\dot{v} = \frac{\partial H}{\partial u}. \tag{2.16}$$

Finally the stationary condition (2.10) can be re-written as

$$\frac{x_0}{b} + \mathrm{i}\frac{p_0}{c} = \frac{q}{b} + \mathrm{i}\frac{p}{c} \tag{2.17}$$

which is equivalent to $u(0) = z$. Therefore, the stationary trajectories are solutions of Hamilton's equations satisfying

$$u(0) = z \qquad \text{and} \qquad X(T) = x_f. \tag{2.18}$$

## 3. Approximations with real trajectories

The stationary phase approximation of the previous section replaces the integral over a continuum of classical real trajectories by a few complex ones. Finding complex trajectories, however, is generally harder than finding real trajectories and one is tempted to look for further approximations to equation (2.14) in terms of real trajectories only. These approximations should be good if the stationary complex trajectory is sufficiently close to a real trajectory.

What real trajectory? According to (2.18), the complex trajectory is determined by two pieces of data: a final position $x_f$ which is real and an initial coordinate $u(0) = z$ which is complex; see (2.17). The latter is made up of a real position $q$ and a real momentum $p$. Thus we have a total of three real parameters, $x_f$, $q$ and $p$ that could be used to determine a real trajectory. Since it actually takes only two parameters, we have three obvious ways of choosing a real trajectory that might sometimes be a good approximation to the complex one. The first way is to give the two initial conditions $(q, p)$, which are the centre of the initial wavepacket in phase space. The other two ways use the final position $x_f$ with a single one of the initial conditions, either $(x_f, q)$ or $(x_f, p)$. Each of these three choices leads to a possible approximation in terms of a real trajectory and, as we shall see, they are all different. In this section we shall derive formulae for each of these three cases. The extent of their validity will be examined in later sections.

We can try to get a rough sense of how close these three real trajectories are to the unique complex one. The latter goes through $x_f$: hence the $(x_f, q)$ and $(x_f, p)$ trajectories have at

least the merit of being at the right position for the final time $T$. To judge the closeness at time 0, we can look at formula (2.14) which tells us that, if $\text{Im}(x_0)$ is sufficiently small compared to $b$, the semiclassical wavefunction at time $T$ will be very small unless $\text{Re}(x_0) - q$ is of order $b$ or smaller. This is a small distance in the semiclassical limit since $b$ is of order $\hbar^{1/2}$. We can also estimate the closeness of the initial momenta by looking at the stationary phase requirement (2.10), separating its real and imaginary parts thus

$$\frac{\text{Re}\, x_0 - q}{b} = \frac{\text{Im}\, p_0}{c} \qquad \frac{\text{Re}\, p_0 - p}{c} = -\frac{\text{Im}\, x_0}{b}. \tag{3.1}$$

Again assuming $\text{Im}(x_0)$ sufficiently small compared to $b$, we see from the second equation that $\text{Re}(p_0) - p$ is of order $c$ or smaller, and $c$ is again proportional to $\hbar^{1/2}$. The conclusion is that a semiclassical approximation in terms of real classical trajectories might be useful if conditions are right.

### 3.1. The central trajectory approximation: Heller's TGA

To begin, we choose the real trajectory defined by the two initial conditions $(q, p)$, the central trajectory of the packet. We call $(q_T, p_T)$ the real end point of this trajectory at time $T$. This trajectory will now be the 0-order approximation. All values of $S$ and its derivatives that occur in the equations, including the $m$ matrix, will be taken for this trajectory, unless we state otherwise explicitly. All these quantities are now real.

We write

$$x_0 = q + \Delta x_i \tag{3.2}$$

$$x_f = q_T + \Delta x_f \tag{3.3}$$

$$p_0 \equiv -\frac{\partial S}{\partial x_i}(x_f, x_0; T) = p + \Delta p_i = p - S_{ii}\Delta x_i - S_{if}\Delta x_f \tag{3.4}$$

$$p_f \equiv +\frac{\partial S}{\partial x_f}(x_f, x_0; T) = p_T + \Delta p_f = p_T + S_{fi}\Delta x_i + S_{ff}\Delta x_f. \tag{3.5}$$

The stationary phase condition (2.10), can be re-written as $\Delta x_i/b + \mathrm{i}\Delta p_i/c = 0$. Then equation (3.4) can be solved for $\Delta x_i$

$$\Delta x_i = -\frac{S_{if}}{S_{ii} + \mathrm{i}c/b}\Delta x_f = \frac{1}{m_{qq} + \mathrm{i}m_{qp}}\Delta x_f. \tag{3.6}$$

To simplify the notation, the complex number $m_{qq} + \mathrm{i}m_{qp}$ will be called $m_+$.

We proceed to expand the exponent in (2.14) about the real trajectory. As before, the pre-factor is assumed to be a slowly varying function and will be simply computed at the real trajectory. We write

$$\frac{\mathrm{i}}{\hbar}S(x_f, x_0; T) + \frac{\mathrm{i}}{\hbar}p(x_0 - q/2) - \frac{(x_0 - q)^2}{2b^2} \approx \frac{\mathrm{i}}{\hbar}S - \frac{\mathrm{i}}{\hbar}p\Delta x_i + \frac{\mathrm{i}}{\hbar}p_T\Delta x_f$$
$$+ \frac{\mathrm{i}}{2\hbar}\left(S_{ii}\Delta x_i^2 + 2S_{if}\Delta x_i\Delta x_f + S_{ff}\Delta x_f^2\right) + \frac{\mathrm{i}}{\hbar}pq/2 + \frac{\mathrm{i}}{\hbar}p\Delta x_i - \frac{\Delta x_i^2}{2b^2}. \tag{3.7}$$

The linear terms in $\Delta x_i$ cancel. The quadratic terms can all be written in terms of $\Delta x_f = (x_f - q_T)$ using (3.6). All second derivatives of the action can be written in terms of the tangent matrix using (2.2). Collecting all quadratic terms we get

$$\frac{i}{2bc}\left(S_{ii}\Delta x_i{}^2 + 2S_{if}\Delta x_i\Delta x_f + S_{ff}\Delta x_f{}^2\right) - \frac{\Delta x_i{}^2}{2b^2}$$

$$= \frac{\Delta x_f{}^2}{2b^2}\left[i\frac{m_{qq}}{m_{qp}}\frac{1}{m_+{}^2} - 2i\frac{1}{m_{qp}}\frac{1}{m_+} + i\frac{m_{pp}}{m_{qp}} - \frac{1}{m_+{}^2}\right]$$

$$= \frac{1}{m_+{}^2 m_{qp}}\frac{\Delta x_f{}^2}{2b^2}\left[im_{qq} - 2i(m_{qq} + im_{qp}) + im_{pp}m_+{}^2 - m_{qp}\right]$$

$$= \frac{1}{m_+{}^2 m_{qp}}\frac{\Delta x_f{}^2}{2b^2}\left[-im_{qq} + m_{qp} + im_{pp}m_+{}^2\right]$$

$$= -\frac{i}{m_+ m_{qp}}\frac{\Delta x_f{}^2}{2b^2}[1 - m_+ m_{pp}] = -\frac{\Delta x_f{}^2}{2b^2}\frac{m_{pp} - im_{pq}}{m_{qq} + im_{qp}} \tag{3.8}$$

where in the last equality we have used $m_{qq}m_{pp} - m_{qp}m_{pq} = 1$.

With these simplifications the semiclassical wavepacket formula becomes

$$\psi_{qp}(x_f, z; T) = \frac{b^{-1/2}\pi^{-1/4}}{\sqrt{m_{qq} + im_{qp}}}\exp\left[\frac{i}{\hbar}S(q_T, q; T) + \frac{ipq}{2\hbar}\right.$$

$$\left. + \frac{i}{\hbar}p_T(x_f - q_T) - \frac{1}{2}\left(\frac{m_{pp} - im_{pq}}{m_{qq} + im_{qp}}\right)\left(\frac{x_f - q_T}{b}\right)^2\right]. \tag{3.9}$$

The subscript $qp$ on $\psi$ indicates the variables used to compute the real trajectory. The spreading of the propagated wavepacket is now explicit in the coefficient of the Gaussian term. This is exactly Heller's thawed Gaussian approximation or TGA [Hel75]. As discussed at the end of section 7, a similar approximation [Bar01] can be obtained with coherent state path integrals.

### 3.2. The approximation by trajectory $q \longrightarrow x_f$

We consider now as 0-order the real trajectory which starts at $q$ and ends at $x_f$ after time $T$. We call $p_i$ its initial momentum, which is a function of $x_f$, $q$ and $T$, and we write

$$x_0 = q + \Delta x_i$$
$$p_0 \equiv -\frac{\partial S}{\partial x_i}(x_f, x_0; T) = p_i + \Delta p_i = p_i - S_{ii}\Delta x_i. \tag{3.10}$$

Note that the complete expansion of $p_0$ to first order should be $p_i - S_{ii}\Delta x_i - S_{if}\Delta x_f$ but, as $x_f$ is fixed, $\Delta x_f = 0$. Equation (2.10) gives us the relation between $\Delta x_i$ and $\Delta p_i$

$$i\frac{(x_0 - q)}{b} = \frac{p_0 - p}{c} = \frac{p_0 - p_i}{c} + \frac{p_i - p}{c}. \tag{3.11}$$

Thanks to equations (3.10) and (3.11) we obtain

$$\Delta p_i = \frac{ic}{b}\Delta x_i - (p_i - p) = -S_{ii}\Delta x_i \tag{3.12}$$

which gives, in terms of the tangent matrix,

$$\Delta x_i = \frac{(p_i - p)}{S_{ii} + \frac{ic}{b}} = \frac{b}{c}\frac{m_{qp}}{m_{qq} + im_{qp}}(p_i - p). \tag{3.13}$$

We expand the exponent of equation (2.14) around this real trajectory. Once again we take the action $S$, its derivatives $S_i$, $S_f$, and its second derivatives $S_{ii}$, $S_{if}$, $S_{ff}$, including the $m$ matrix,

for the 0-order trajectory, unless we state otherwise explicitly. We obtain

$$
\frac{i}{\hbar} S(x_f, x_0; T) + \frac{i}{\hbar} p(x_0 - q/2) - \frac{(x_0 - q)^2}{2b^2}
$$

$$
= \frac{i}{\hbar} \left( S + S_i \Delta x_i + \frac{1}{2} S_{ii} \Delta x_i^2 \right) + \frac{i}{\hbar} p \Delta x_i + \frac{i}{2\hbar} pq - \frac{\Delta x_i^2}{2b^2}
$$

$$
= \frac{i}{\hbar} S + \frac{i}{2\hbar} pq + \frac{i}{\hbar}(p - p_i) \Delta x_i + \frac{1}{2} \left( \frac{i S_{ii}}{\hbar} - \frac{1}{b^2} \right) \Delta x_i^2
$$

$$
= \frac{i}{\hbar} S + \frac{i}{2\hbar} pq - \frac{i m_{qp}}{m_{qq} + i m_{qp}} \frac{(p_i - p)^2}{c^2} + \frac{1}{2} \frac{i m_{qp}}{m_{qq} + i m_{qp}} \frac{(p_i - p)^2}{c^2}. \tag{3.14}
$$

Finally, the semiclassical propagator as a function of $q$, $p$, $x_f$ and $p_i$, becomes

$$
\psi_{x_f q}(x_f, z; T) = \frac{b^{-1/2} \pi^{-1/4}}{\sqrt{m_{qq} + i m_{qp}}} \exp \left[ \frac{i}{\hbar} S(x_f, q; T) + \frac{i}{2\hbar} pq \right.
$$

$$
\left. - \frac{1}{2} \frac{i m_{qp}}{m_{qq} + i m_{qp}} \left( \frac{p - p_i}{c} \right)^2 \right]. \tag{3.15}
$$

The Gaussian in the exponent is now in the difference between $p_i$, the initial momentum of the real trajectory and $p$, the initial momentum of the centre of the wave packet. Note that there might be more than one trajectory satisfying the boundary conditions $X(0) = q$, $X(T) = x_f$. Note also that the wavefunction is no longer restricted to a Gaussian, and that this is *not* an initial value formula.

### 3.3. The approximation by trajectory $p \longrightarrow x_f$

In the same way, if we choose as 0-order the trajectory specified by $p$ and $x_f$ instead of $q$ and $x_f$, we call $q_i$ the initial position for this trajectory, which is a function of $x_f$, $p$ and $T$, and we write

$$
\begin{aligned}
x_0 &= q_i + \Delta x_i \\
p_0 &\equiv -\frac{\partial S}{\partial x_i}(x_f, x_0; T) = p + \Delta p_i = p - S_{ii} \Delta x_i.
\end{aligned} \tag{3.16}
$$

Thanks to equations (2.10) and (3.16) the new expression for $\Delta x_i$ is

$$
\Delta x_i = \frac{i m_{qp}}{m_{qq} + i m_{qp}}(q - q_i). \tag{3.17}
$$

In the end we obtain a propagating semiclassical wavepacket different from the other two, namely

$$
\psi_{x_f p}(x_f, z; T) = \frac{b^{-1/2} \pi^{-1/4}}{\sqrt{m_{qq} + i m_{qp}}} \exp \left[ \frac{i}{\hbar} S(x_f, q_i; T) + \frac{i}{2\hbar} pq \right.
$$

$$
\left. + \frac{i}{\hbar} p(q_i - q) - \frac{1}{2} \frac{m_{qq}}{m_{qq} + i m_{qp}} \left( \frac{q - q_i}{b} \right)^2 \right]. \tag{3.18}
$$

The Gaussian in the exponent is in the difference between $q_i$, the initial position of the real trajectory, and $q$, the initial position of the centre of the wavepacket. This formula shares many of the features of the previous one, including not being a Gaussian and not being an initial value formula.

The three real trajectory approximations we derived here are formally similar. Among the three real variables $q$, $p$ and $x_f$, two are chosen to fix the trajectory. Then the corresponding formula carries a Gaussian damping factor in the third variable. In the next three sections we discuss some examples that will help us compare these approximations with $\psi_{CT}$ which involves complex trajectories. As usual all these formulae are exact for the free particle and the harmonic oscillator.

## 4. First applications: the free particle and the hard wall

The exact result for the propagation of a free particle wavepacket is of course well-known, but it can serve as a test of the formulae of sections 2 and 3. And it is instructive to be able to see explicitly the different trajectories involved in each approximation. The wavefunction for the packet at time 0 is given by (2.4). The Hamiltonian is simply $H = P^2/2\mu$ where $\mu$ is the mass. The action is

$$S(x_f, x_i; T) = \frac{\mu}{2} \frac{(x_f - x_i)^2}{T}. \tag{4.1}$$

All trajectories have constant momentum or velocity. In addition to the other parameters we shall use $\omega = c/\mu b = \hbar/\mu b^2$, which is the frequency of the oscillator upon which the coherent states are built, and $v = p/\mu$, the central velocity of the wavepacket. The elements of the tangent matrix are $m_{qq} = 1$, $m_{qp} = \omega T$, $m_{pq} = 0$, $m_{pp} = 1$.

The exact expression for the propagated wavepacket follows from elementary quantum mechanics and can be written

$$\psi_{\text{exact}}(x_f, z; T) = \frac{1}{b^{1/2}\pi^{1/4}} \frac{1}{\sqrt{1 + i\omega T}}$$
$$\times \exp\left[-\frac{(x_f - q - vT)^2}{2b^2(1 + \omega^2 T^2)}(1 - i\omega T) + \frac{i}{\hbar}p\left(x_f - \frac{q}{2} - \frac{vT}{2}\right)\right]. \tag{4.2}$$

It describes a Gaussian packet of constant momentum $p$, whose real width $b\sqrt{1 + \omega^2 T^2}$ increases with time, but whose total width is actually complex and given by $b\sqrt{1 + i\omega T}$.

For the approximation of section 2, the stationary point $x_0$ of the integration, which is the origin of the complex trajectory, and its associated momentum $p_0$, which is the constant momentum of the trajectory, turn out to be

$$x_0(x_f, z; T) = \frac{x_f + i\omega T\left(q + i\frac{b}{c}p\right)}{1 + i\omega T} \qquad p_0(x_f, z; T) = \frac{p + i\frac{c}{b}(x_f - q)}{1 + i\omega T}. \tag{4.3}$$

One can check the two boundary conditions (2.18)

$$\frac{x_0}{b} + i\frac{p_0}{c} = \frac{q}{b} + i\frac{p}{c} \qquad x_0 + \frac{p_0}{\mu}T = x_f. \tag{4.4}$$

One can also verify that, when $x_f$ has the value $q + vT$, one finds the simple answers $x_0 = q$ and $p_0 = p$: the trajectory is just the central trajectory of the packet.

Let us look also at the three approximations with real trajectories. For the $(q, p)$ case, formula (3.9) contains both $q_T$ and $p_T$. The former is clearly $q_T = q + vT$, while $p_T = p$, the constant momentum. For $(x_f, q)$, formula (3.15), we need $p_i$ which is $p_i = \mu(x_f - q)/T$. We do not need $p_f$, but it is obviously the same as $p_i$. Finally, for $(x_f, p)$, formula (3.18), we need $q_i = x_f - pT/\mu$, since the constant momentum is $p$. Once again, for the free particle, all four semiclassical approximations give the exact answer.

To make things less trivial, we shall now have the wavepacket bounce elastically against a hard wall placed at the origin. The packet arrives from the right with a negative momentum

and we assume that it starts far enough to have no appreciable value at the wall at time 0. The only relevant spatial region is $x_f > 0$; the other side of the wall does not exist for this problem. Of course the wall could be an approximation to a very steep, but not totally hard, potential, in which case there would be some barrier penetration to the other side. And it would be interesting to see what happens in the limiting process, but we shall not do that here.

The exact solution is quite simple, once one knows the exact free particle formula (4.2): you take the $x_f < 0$ part of the latter, you reflect it with respect to the wall and you give it an additional minus sign. Thus the complete solution has two parts, both restricted to $x_f > 0$, the original free particle part, and the reflected part which uses the $x_f < 0$ piece of the free particle:

$$\psi_{\text{wall, exact}}(x_f, z; T) = \psi_{\text{free, exact}}(x_f, z; T) - \psi_{\text{free, exact}}(-x_f, z; T)$$
$$x_f > 0 \text{ only}, \qquad T > 0. \tag{4.5}$$

This construction ensures that the Schrödinger equation is satisfied everywhere and that the total wavefunction vanishes at the wall.

Next we look at the semiclassical approximation with complex trajectories, section 2. Given $x_i$ and $x_f$, both $>0$, there are two ways to go from one to the other in time $T$, the direct way and the way which bounces off the wall. The first trajectory is identical in all respects to a free particle's: it has the same action (4.1) and the process of finding the stationary point $x_0$ of the integration over $x_i$ is the same. Hence, for this direct trajectory, formula (2.14) yields the free particle result, restricted to $x_f > 0$. The reflected trajectory, on the other hand, has a different action. The distance between $x_i$ and $x_f$, including reflection, is $D = x_f + x_i$, the speed is $(x_f + x_i)/T$, the momentum $\mu(x_f + x_i)/T$ and the energy $\mu(x_f + x_i)^2/2T^2$. Hence the action is

$$S(x_f, x_i; T) = PD - ET = \mu \frac{x_f + x_i}{T}(x_f + x_i) - \frac{\mu}{2}\frac{(x_f + x_i)^2}{T^2}T = \frac{\mu}{2}\frac{(x_f + x_i)^2}{T}. \tag{4.6}$$

It differs from (4.1) by a sign change for one of the two coordinates. The initial and final momenta follow from this action in the usual way:

$$p_f = \frac{\partial S}{\partial x_f} = \mu \frac{x_f + x_i}{T} \qquad p_i = -\frac{\partial S}{\partial x_i} = -p_f. \tag{4.7}$$

Compared to the direct trajectory, the only change that needs to be made when we look for the stationary point of the $x_i$ integration and we apply formula (2.14), is that the constant quantity $x_f$ must be replaced everywhere by $-x_f$. Thus we get again the free particle result, but for the value $-x_f$ of the position. This approximation, therefore, yields the exact answer (4.5), except for the minus sign in front of the second term. This minus sign due to reflection is expected on very general grounds. It is a special case of the Morse phase mentioned in section 2, and it is understood easily if one looks at a soft barrier, such as a finite square step, and one goes to the infinite limit.

Now let us try to apply to the hard wall the approximation with the $(q, p)$ real trajectory of section 3.1. We shall see that it does not work for this kind of problem. In this formulation there is a single trajectory, which begins at $(q, p)$ and evolves with $T$. Its endpoint is given by $q_T = q - |v|T$ until it hits the wall, which happens for time $T_r = q/|v|$. After this time $q_T$ becomes $|v|T - q$. Formula (3.9) yields for a given $T$ a single Gaussian wavepacket whose centre follows this trajectory. The packet is incoming for $T < T_r$ and outgoing for $T > T_r$. Incoming and outgoing are never present at the same time and therefore there are no interference effects. In a calculation for a soft wall, one would see the full amplitude of the Gaussian packet on the back side of the wall, with no damping due to barrier penetration, and again no interference effects.

On the other hand, the other two approximations with real trajectories, $(x_f, q)$ and $(x_f, p)$, do work fine for the hard wall and give the exact answer. Each of them contains a direct and a reflected trajectory at all times, hence a sum of two wavepackets with interference.

## 5. The inverted Gaussian potential

The hard wall is probably the simplest example after the free particle. However, except for $\psi_{qp}$, the calculation involves two trajectories. Our aim here is to consider a potential where a single classical trajectory contributes to the semiclassical formulae, to avoid dealing with interference and focus only on the differences arising from the complex or real character of a trajectory. We choose an inverted Gaussian potential with Hamiltonian

$$H(X, P) = \frac{P^2}{2} - e^{-X^2}. \tag{5.1}$$

The system has a single parameter, which is the width of the wavepacket. We set $\hbar = 1$ and place the packet initially at $q = -5$, $p = 1/2$, hence central energy $1/8$. There is a single bound level with energy $-0.48$, which excludes two simple limits: that in which the potential is just a perturbation, and that in which the problem is highly semiclassical. Here both the real and the complex trajectories need to be calculated numerically, as well as the exact packet propagation of course. The numerical methods for the trajectories will be discussed in the next section.

Figure 1 shows the wave packet at $T = 7$ for the different approximations, compared with the exact result, for two values of the width, $b = 0.5$ and $b = 1.0$. The packet spreads very fast and rapidly becomes highly non-Gaussian. It is remarkable how well this non-Gaussian character is reproduced by some of the approximations, though not all. We shall have more to say in section 7 about comparing the various approximations. The top two graphs are the probability density versus $x_f$. The bottom two are the phase of the wavefunction. Both the modulus and the phase are very well reproduced by $\psi_{CT}$, the approximation via complex trajectories, and $\psi_{x_f q}$, one of the real trajectories approximations, $\psi_{x_f q}$ being just as good as $\psi_{CT}$ for this. On the other hand $\psi_{qp}$, which is a pure Gaussian, does not do well at all. The small zig-zags in the approximate calculations of the phase are due to numerical imprecisions. Here, as well as in the next section, we do not show $\psi_{x_f p}$, because it displays basically the same features as its counterpart $\psi_{x_f q}$. Calculations with other values of $b$ show these results to be robust, in the sense that $\psi_{x_f q}$ is always very similar to $\psi_{CT}$ and that both agree well with the exact propagation.

## 6. The quartic oscillator

In this section we apply our semiclassical formulae to the case of a totally binding potential. We choose the quartic oscillator because it is probably the simplest system after the harmonic oscillator (for which all semiclassical formulae of sections 2 and 3 are exact). The Hamiltonian is

$$H = \frac{P^2}{2} + AX^2 + BX^4 \tag{6.1}$$

and the parameters are set to $A = 0.5$, $B = 0.1$, $\hbar = 1$. For these values the ground state energy is $E_0 \approx 0.559$ and the first two excited states have $E_1 \approx 1.770$ and $E_2 \approx 3.319$. For the wavepacket we choose $q = 0$, $p = -2.0$ and $b = 1.0$. This gives $E = H(q, p) = 2.0$ for the energy of the central trajectory, $\tau \approx 4.7$ for its period and $X_{\text{turn}} \approx \pm 1.6$ for its
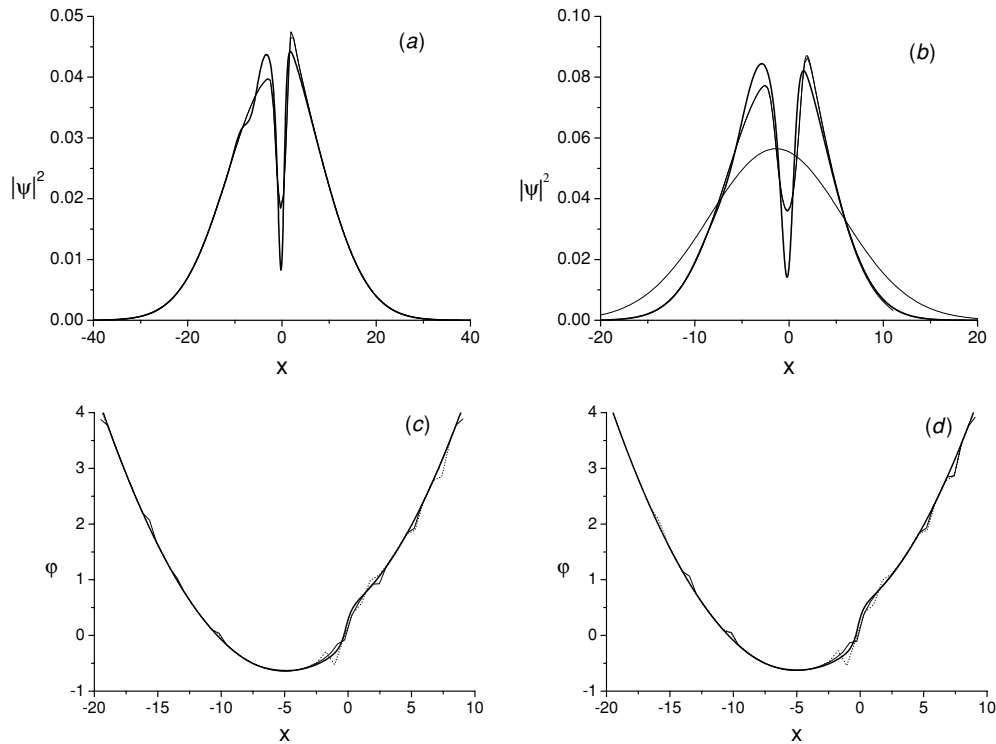
**Figure 1.** Parts (*a*) and (*b*) show the probability density in the inverted Gaussian potential for $p = 0.5$ and $T = 7.0$. In (*a*) $b = 0.5$ and in (*b*) $b = 1.0$. The thick solid line shows the exact result, the thin solid line corresponds to $\psi_{CT}$ and the dotted line to $\psi_{x_f q}$ (which cannot be distinguished from $\psi_{CT}$ at this scale). Part (*b*) also shows a comparison with $\psi_{qp}$ (symmetric Gaussian curve). Parts (*c*) and (*d*) show the phase of the wave packet, in units of $\pi$, corresponding to (*a*) and (*b*) respectively. In this figure and those following, the *x* variable in the abscissa is actually the variable $x_f$ of the text.

turning points. Figure 2 shows a sequence of four snapshots in the exact time evolution of the packet. The energy is low, the wavelength is large and the interference effects are important.

As in the previous example, both the real and the complex trajectories have to be computed numerically. The real trajectories from $q$ to $x_f$ can be calculated with a simple 'shooting method'. Since we need the propagated wave packet at all values of $x_f$, we simply integrate the equations of motion starting from $X(0) = q$ (fixed) and several values of the initial momentum $P(0) \equiv p_i$. For each $p_i$ we obtain a final coordinate $X(T) \equiv x_f$ at which we evaluate the wavefunction.

The calculation of the complex trajectories is more involved and we shall describe it in some detail. We follow the procedure introduced by Klauder [Kla87] (see also [Hel87, Ada89, Rub95] and [Rib04] for a different approach), which consists in propagating trajectories starting from

$$X(0) = q + w \qquad P(0) = p + i\frac{c}{b}w \tag{6.2}$$

where $w \equiv \alpha + i\beta$ is a complex number. The first of conditions (2.18) is automatically satisfied for all $w$. The search method consists in propagating trajectories for all possible $w$ and picking those satisfying the second condition (2.18), $X(T) = x_f$.
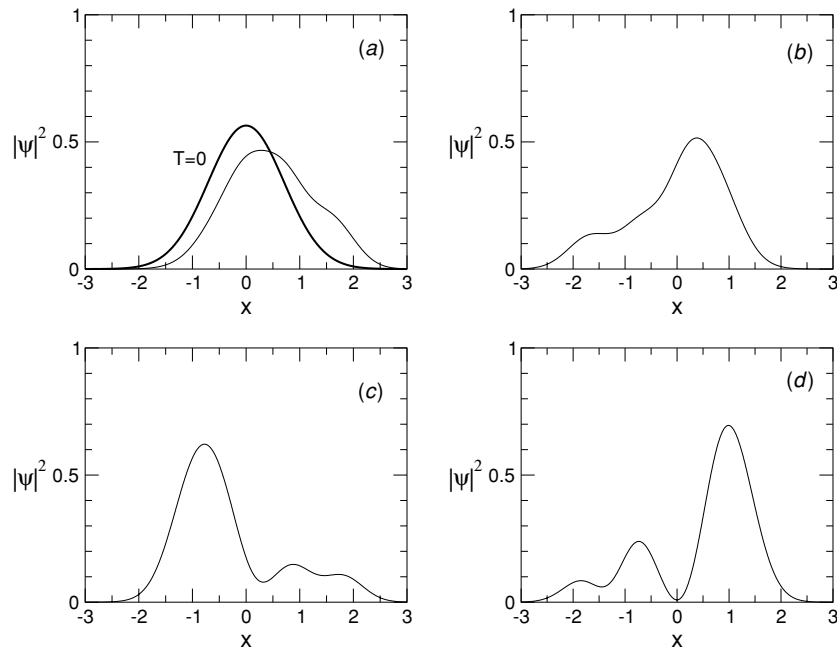
**Figure 2.** Exact quantum mechanical propagation in the quartic potential with $A = 0.5$, $B = 0.1$ and $\hbar = 1$. The wavepacket is initially centred at $q = 0$, $p = -2$ and has width $b = 1$. The curves show the probability density at times (a) $T = 0$ (thick line) and $T = 2.5$, (b) $T = 4.5$, (c) $T = 6.5$ and (d) $T = 8.5$. The period of the classical orbit of the centre of the packet is $\tau \approx 4.7$.

As discussed in [Rub95], fixing $q$, $p$ and $T$ and integrating Hamilton's equations with initial conditions (6.2) gives, for each $w$, a final coordinate $X(T) \equiv X_T$, usually complex. This can be viewed as a map $X_T = X_T(w)$. The values of $w$ we need are given by the inverse map of the real $X$ axis. If the map is analytic at $w$, then it is conformal. This implies, among other things, that the map is one-to-one in the neighbourhood of $w$. If, on the other hand, $w$ is a critical point of the map, a richer structure develops. If, for instance, $\partial X_T / \partial w = 0$, but the second derivative is non-zero, it can be shown that the map becomes two-to-one in the vicinity of $w$, meaning that two different trajectories (corresponding to two distinct initial conditions) satisfy the same boundary conditions. This is the basic mechanism that generates multiple trajectories in systems with one degree of freedom. For short times the critical points of the map generically lie very far from the origin $w = 0$, corresponding to complex trajectories whose actions have large imaginary parts. As time increases, more and more of these points approach the origin, giving rise to significant contributions to the propagator [Rub95]. The singularities in the $X_T(w)$ map produced by the critical points are called phase space caustics (PSC). At these points the square-root in the pre-factor of equation (2.14) goes to zero and the semiclassical approximation fails (it actually fails in a finite neighbourhood of the PSC's).

For fixed $q$, $p$ and $T$, the complex trajectories form continuous families parametrized by $x_f$. Among the many families that might contribute to the semiclassical evolution of the wave-packet, one is special. This is the family that contains the real trajectory that starts at $(q, p)$, and we call it the *main family*. If $(q_T, p_T)$ is the end point of this real trajectory, then for $x_f = q_T$ the trajectory in the main family is real. In terms of the map, the point $w = 0$ is mapped into $X_T = q_T$. In some special situations, the main family alone may provide
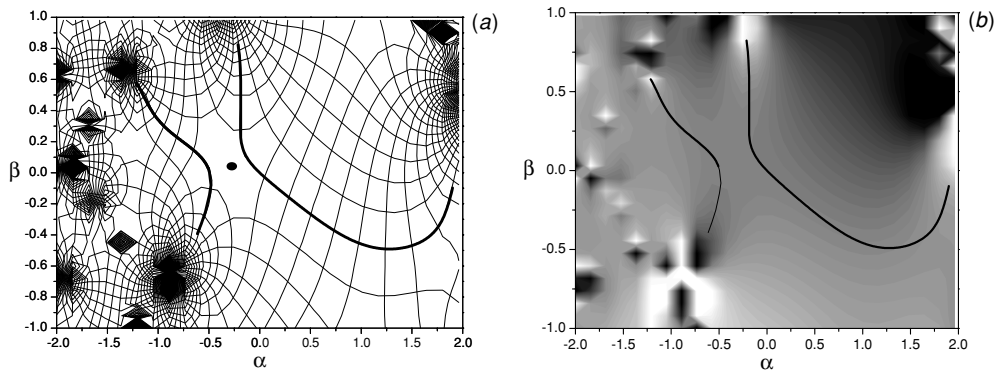
**Figure 3.** (*a*) Map $X_T = X_T(w)$ for $T = 6.5$. The lines correspond to constant values of Re($X$) and Im($X$) and the circle indicates the singularity. The thick lines correspond to the trajectories satisfying Im($X_T$) = 0; (*b*) greyscale topographic plot of the imaginary part of the exponent $F$ for all the trajectories in (*a*). The shades of grey go from $-\infty$ (black) to $+\infty$ (white). The main family has Im($F$) $\geqslant 0$ whereas the secondary family has a section where Im($F$) < 0 (thin line).

sufficient information for the semiclassical calculation [Hel87, Hel02, Hel03], but that is not always the case [Shu95, Shu96, Rib04].

Figure 3(*a*) shows the map $X_T = X_T(w)$ for $T = 6.5$. The lines correspond to constant values of Re($X$) and Im($X$). The conformal property of the map guarantees that these lines cross at right angle (provided the same scale is used for $\alpha$ and $\beta$). The circle indicates the location of a critical point, corresponding to a singularity in the regular pattern of the lines. The thick lines correspond to families of trajectories for which Im($X(T)$) = 0. The main family can be identified by its containing the point $w = 0$. A more careful look at this figure reveals the existence of several other singularities in the otherwise regular pattern of crossing lines. Each of them is a critical point of the map. The trajectories in their neighbourhood, however, do not contribute significantly to the propagated wave packet, and we shall not take them into account.

Let

$$F \equiv S(x_f, x_0; T) + p(x_0 - q/2) + i\hbar \frac{(x_0 - q)^2}{2b^2} \tag{6.3}$$

be the exponent in equation (2.14). For real trajectories Im($F$) is $\geqslant 0$. Figure 3(*b*) shows a greyscale topographic map of Im($F$) for the trajectories calculated in figure 3(*a*) and in the same ($\alpha, \beta$) plane. The continuous thick line is the main family seen on figure 3(*a*). The line for the other family, which we call *secondary*, is partly thick and partly thin. The reason for this distinction is the following. The imaginary part of $F$ for trajectories in the main family can be seen to be always positive. It starts with Im($F$) = $+\infty$ for $x_f = +\infty$, decreases to zero at $x_f = q_T$ and grows to infinity again as $x_f \to -\infty$. For the trajectories in the secondary family, however, Im($F$) starts at $+\infty$ for $x_f = +\infty$, and decreases steadily to Im($F$) = $-\infty$ at $x_f = -\infty$. This means that this family cannot be included in the semiclassical calculation for all values of $x_f$. There must be a cutting point after which the family cannot be considered, otherwise it would cause the wavefunction to diverge. This phenomenon has become known as the *problem of non-contributing trajectories*, and has been studied by Adachi [Ada89], Berry [Ber89], Klauder [Rub95] and others [Shu95, Shu96, Tan98, Rib04]. The part of the secondary family shown with the thin line has not been included in our calculations. We note
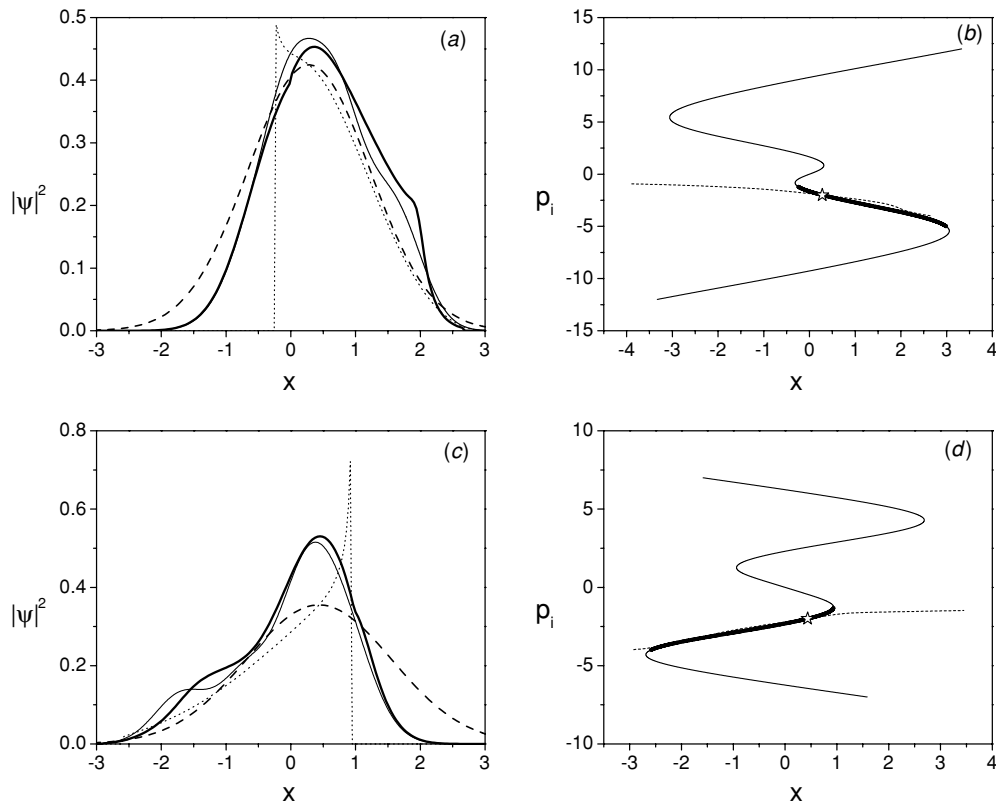
**Figure 4.** Parts ($a$) and ($c$) show the probability density in the quartic potential for $T = 2.5$ and $T = 4.5$ respectively. The thin solid line shows the exact result, the dotted line corresponds to $\psi_{x_f q}$, the dashed line to $\psi_{qp}$ and the thick solid line to $\psi_{\mathrm{CT}}$. Parts ($b$) and ($d$) show the initial momentum $p_i$ as a function of $x$ for the ($q, x$) real trajectory for $T = 2.5$ and $T = 4.5$. The thick line shows the branch used in the calculation of $\psi_{x_f q}$ and the star represents the central trajectory starting from $q, p$. The dashed line corresponds to the projection of the main family of complex trajectories into this real plane.

that, in [Hel87], Huber and Heller do a similar calculation for a wave packet moving in the Morse potential.

To understand qualitatively the role of secondary families in the semiclassical limit, we consider $\hbar$ to be really very small. In this case the ($x_f, q$) and ($x_f, p$) real trajectory approximations of section 3 become exact, and only the main family (actually only a small neighbourhood of the real trajectory) contributes significantly. Demanding the approximation to be uniformly valid as $\hbar \to 0$, and using the subscript $m$ for the main family and $s$ for a secondary one, we must apply the following rules: ($a$) trajectories with $\mathrm{Im}(F_s) < 0$ should be removed [Rub95]. This avoids the divergence of $\exp\{\mathrm{Im}(F_s)/\hbar\}$ in the limit $\hbar \to 0$; ($b$) trajectories with $\mathrm{Im}(F_s)(x_f) > 0$ but $\mathrm{Im}(F_s(x_f)) < \mathrm{Im}(F_m(x_f))$ should also be removed to guarantee that, as $\hbar \to 0$, the main family always gives the dominant contribution; and ($c$) the discontinuity introduced by the sudden removal of a secondary contribution should be minimized. This criterion ultimately determines the choice of the cutoff point, which is located on the so-called Stokes line [Rub95].

Figure 4 shows the comparison between the exact calculation (thick line) and the different approximations of sections 2 and 3 for $T = 2.5$ and $T = 4.5$. The most interesting feature
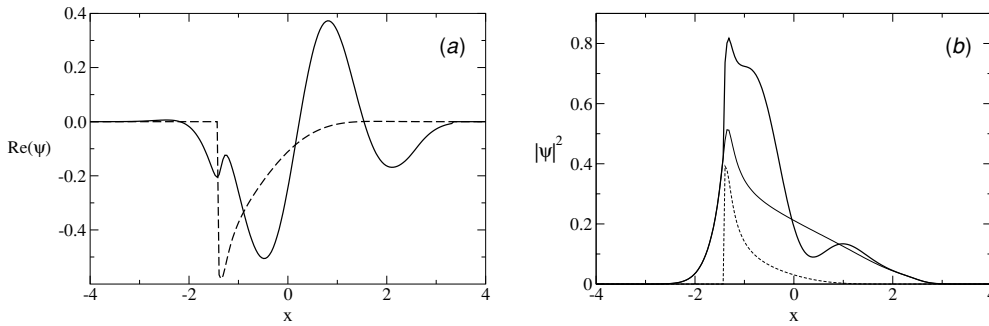
**Figure 5.** Separate contributions of the main (solid line) and secondary (dashed line) families for the wave packet at $T = 6.5$. (*a*) Real part of $\psi$; (*b*) probability density $|\psi|^2$. Note the abrupt cutoff of the secondary family. The thick line in (*b*) shows the total probability density, displaying the interference between the individual contributions.

here is that the real trajectory formula $\psi_{x_f q}$ becomes discontinuous. This can be understood with the help of panels (*b*) and (*d*) which show the initial momentum $p_i$ of the contributing trajectories as a function of $x_f$ (for fixed $q$ and $T$). We see that several branches appear, but it turns out that only that shown with a thick line contributes significantly. Since this main branch covers only a finite range of $x_f$, the wavefunction drops to zero suddenly. In fact, the wavefunction diverges at the ends of the branches. In our calculations we have cut the branch a little before its end points.

Figure 5(*a*) shows the real part of $\psi_{\text{CT}}(x_f, z; T)$ for $T = 6.5$ calculated with the separate contribution of each of the families shown in figures 3. The abrupt cutoff of the secondary family is clear in this figure. Figure 5(*b*) shows again the separate contributions of the same families to $|\psi_{\text{CT}}(x_f, z; T)|^2$ (dashed and solid lines) and their combined contribution (thick solid line). Note the interference between the two families producing the oscillation in the probability density.

Finally figure 6 shows $|\psi_{\text{CT}}(x_f, z; T)|^2$, the calculation with complex trajectories. Each snapshot shows the exact result (thin solid line), the thawed Gaussian approximation $\psi_{qp}$ (dashed line) and the complex trajectories approximation (thick line). We do not show $\psi_{x_f q}$ in these plots because the approximation is not good. The improvement obtained with the complex trajectories is clear. For $T = 6.5$ and $T = 8.5$, however, we can see a spurious peak close to the turning points. This might seem to result from cutting off the secondary family at the wrong point, as suggested in [Hel88]. A careful analysis shows that it is not the case: cutting off the secondary family at a smaller value of $x_f$ would produce a sudden dip in the probability density followed by another sudden increase, as can be seen from figure 5(*b*). The spurious peaks are due to the phase space caustic that shows up close to the turning points. For the present situation, which is not quite in the semiclassical domain, the caustics have a strong effect on the semiclassical propagations and further corrections are necessary to improve the approximation. A uniform semiclassical approximation involving Airy functions can be derived by considering cubic terms in the saddle point approximation performed in integral (2.5). The derivation of this improved formula will be published elsewhere.

## 7. Summary and discussion

We begin by summarizing the results. We have derived and written down in this paper (sections 2 and 3) four semiclassical expressions for the propagation of an initially Gaussian
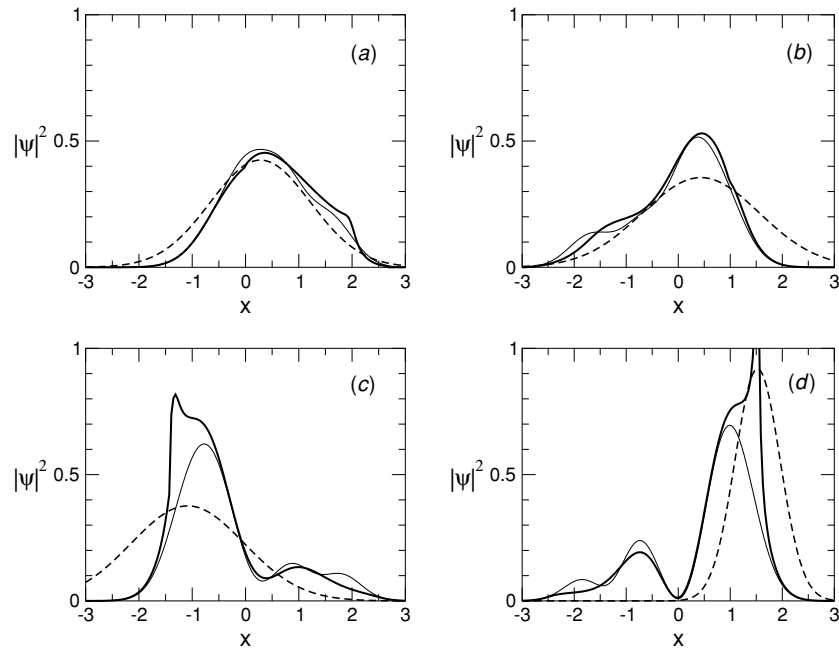
**Figure 6.** Probability density for the quartic potential for (*a*) $T = 2.5$; (*b*) $T = 4.5$; (*c*) $T = 6.5$ and (*d*) $T = 8.5$. The thin solid line shows the exact result, the dashed line corresponds to $\psi_{qp}$ and the thick solid line to $\psi_{CT}$.

wavepacket, $\psi_{CT}$, $\psi_{qp}$, $\psi_{x_f q}$, $\psi_{x_f p}$. All four give exact results for the free particle and the harmonic oscillator. All except $\psi_{qp}$ also give the exact result for the scattering by a hard wall. But $\psi_{qp}$ is very bad for the hard wall: it produces no interference. We tested the formulae further on two examples of smooth potentials. For the attractive Gaussian potential, the exact packet after some time is highly non-Gaussian. Both $\psi_{CT}$ and $\psi_{x_f q}$ involve a single trajectory for each $x_f$, and both give very good results for the modulus as well as the phase of the wave packet. The same is true of $\psi_{x_f p}$. But $\psi_{qp}$, which is a pure Gaussian, gives a very bad fit.

The other smooth potential is a quartic oscillator. Now there may be contributions from multiple families of trajectories and the results are quite different. We found in this case that the complex trajectories formula $\psi_{CT}$ is superior to both the real trajectories approximation $\psi_{x_f q}$ and the single trajectory approximation $\psi_{qp}$. One reason is that the real trajectories contributing to $\psi_{x_f q}$ have finite branches, which causes a drastic discontinuity in the approximate wavefunction. The complex trajectories, on the other hand, form continuous branches that prolong into the complex domain. The projection of these complex families onto the real plane show that they follow closely the main branch of the real trajectories, but they continue to exist after the latter end.

Thus the paper's main finding is that the complex trajectory approximation, $\psi_{CT}$ of equation (2.14), gives very good results, at least for all the cases that we looked at. And one may well wonder how it could be that a relatively simple approximation, based on a single trajectory, works so well. The short answer is that, actually, the approximation is not that simple and it is not based on a single trajectory. But we shall go into more details.

Many other approaches have been proposed for the propagation of an initial wavefunction, some of them especially concerned with the propagation in systems with many degrees of

freedom. Among them, initial value representations (IVRs) [Mill74, Her84, Hel91, Kay94a, Pol03, Tho04] have become especially popular. They are integral expressions over the phase space of initial conditions, in a spirit which tends to rejoin that of path integrals. The multiple integration is usually handled by Monte Carlo techniques [Kay94b, Zha03]. The initial impetus for these approaches [Mill70] was the root-search problem, i.e. the fact that the Van Vleck expression (2.3) requires one to find trajectories determined by mixed initial–final boundary conditions (starting at $x_i$ and ending at $x_f$). This may lead to a difficult search in complicated situations, and in addition the root-search problem usually has several solutions, a fact which complicates further the time development of the wavefunction. In the IVRs, on the other hand, the trajectories are determined solely by initial boundary conditions, as the name implies, and for each set of initial conditions there is only one trajectory, the unique solution of Hamilton's equations for these conditions. The work of getting the correct propagated wavefunction is done entirely by the integration, as is the case for path integral expressions.

The present work is based on the Van Vleck expression and it is affected by root search, except for the thawed Gaussian formula $\psi_{qp}$ of section 3.1. Root search can truly be a burden, especially for multi-dimensional wavefunctions. More important, however, is the fact that characterizing the present approach as a one-trajectory or a few-trajectories approximation is highly misleading. We have used such characterization several times above, for instance in connection with the hard wall, or in the first few lines of section 5. But the truth is that there is a different classical trajectory for every final $x_f$, and therefore the number of trajectories is really infinite. The work of getting the correct propagated wavefunction is done by them.

The one case where we truly have a one-trajectory expression is $\psi_{qp}$. There, the same trajectory is used for all values of $x_f$. This case is truly an IVR, though a very simplified one, not involving any integration over the initial parameters. The only initial parameters used are those of the centre of the packet. And it is also the case for which, in our explorations, the agreement with the exact result is worst, showing that a single classical trajectory is just not enough. Somehow, a variety of classical trajectories must enter into the formalism. In other words, we see the path integral idea reappear, Feynman's original view of the connection between quantum and classical mechanics.

Among the various IVRs, there is one that has been especially successful and has had many applications, the Herman–Kluk approximation [Her84, Kay94a, Gar00, Wan01, Noi03]. It would be particularly interesting to have a direct application of the HK formula to the hard wall, since this is the simplest non-obvious case for which our complex trajectories formula is exact. We are not aware of the existence of such an application of HK, and it seems to us that the calculation will not be totally straightforward.

Perhaps it is not superfluous to repeat once again that the main new result of this paper is that semiclassical approximations using complex trajectories, especially non-IVR approximations, are capable of being surprisingly good. All our semiclassical expressions generalize easily to many dimensions. The detailed presentation of these generalizations will be published separately, together with numerical applications. We note that two-dimensional semiclassical calculations with complex trajectories have already been considered in the context of coherent states. In [Hel02, Rib04] the quantity evaluated was the return probability amplitude, also known as the auto-correlation function. In [Shu95, Shu96, Oni01] the authors, who seem to have been unaware of [Hel87, Hel88], calculate the propagated wavefunction in the momentum or coordinate representation. But they do it for quantum maps, which is rather different from what we have done here since, in their case, there are no continuous classical trajectories, no Hamilton equations and no Schrödinger equation. In this paper we provided formulae for the calculation of the propagated wavefunction for continuous systems in the coordinate representation. The basic equation for such calculations is the complex

trajectory formula (2.14) first derived by Heller and coworkers in [Hel88]. We showed that one can approximate the complex trajectories by real ones, and that this can be done in various ways (we mention three of them), with different degrees of difficulty and of accuracy. The various formulae so generated will undoubtedly have different domains of applicability. And the complex formula, if it is practical, will always remain the better one.

As our final topic, we shall present an alternative derivation of a formula very similar to (2.14), which possesses the same three approximations in terms of real trajectories. The quantity we want to calculate is $\langle x_f | K(T) | z \rangle$. To obtain the approximation (1.6), we introduced between $K(T)$ and $|z\rangle$ the resolution of unity in terms of eigenstates of $x$, and then we replaced the exact $x$-propagator by its Van Vleck approximation. Instead of this, we shall introduce between $\langle x_f |$ and $K(T)$ the resolution of unity in terms of coherent states, thus

$$\langle x_f | K(T) | z \rangle = \int \langle x_f | z' \rangle \frac{\mathrm{d}^2 z'}{\pi} \langle z' | K(T) | z \rangle \tag{7.1}$$

and then we shall replace the exact coherent state propagator by its semiclassical approximation. The latter was worked out in detail in [Bar01]. Performing the integrals over $q'$ and $p'$ by the stationary exponent approximation, we arrive at an expression which is very similar, but not identical, to (2.14). There are two important differences. One is that, in this case, the dynamics are governed by the smoothed Hamiltonian $\mathcal{H}(q, p) = \langle z | H | z \rangle$ instead of the classical Hamiltonian. The other is that the exponent acquires an extra term given by [Bar01]

$$\frac{\mathrm{i}}{\hbar} \mathcal{I} \equiv \frac{\mathrm{i}}{\hbar} \int_0^T \mathrm{d}t \left( \frac{b^2}{4} \frac{\partial^2 \mathcal{H}}{\partial q^2} + \frac{c^2}{4} \frac{\partial^2 \mathcal{H}}{\partial p^2} \right). \tag{7.2}$$

This term plays a very important role and cannot be dropped from the approximation. Both $\mathcal{I}$ and the $\mathcal{H}$ dynamics get carried over into all the real trajectories approximations.

Our main reason for mentioning this alternative is to stress that semiclassical approximations are never unique and that there are always many ways to base an approximate quantal expression on a classical solution. Discussions of this appear in [Kla85], who see it as a consequence of the over-completeness of the coherent-state basis, and also in [Bar01]. It is only in the limit of $\hbar$ going to zero that they all become the same. From our alternative to (2.14) involving the smoothed Hamiltonian and the correction term $\mathcal{I}$, one can derive again three expressions in terms of real trajectories, different from those in section 3. Numerically, the two points of view yield roughly equally good (or sometimes equally bad) results. And once again, for quadratic Hamiltonians, all the approximations we have mentioned are exact. While in section 3 the $\psi_{qp}$ approximation was the same as Heller's TGA, for the alternative formulation it is the same as the approximation in section 4 of [Bar01]. The latter reference contains a discussion of the differences between the two results. Both are initial value formulae using the real central trajectory of the packet, and both are Gaussian in shape for all potentials and all times. Both are expected to fail if the potential is not very smooth on the scale of the size of the packet.

## Acknowledgments

## References

[Ada89]  Adachi S 1989 *Ann. Phys. NY* **195** 45
[And98]  Andrews M 1998 *Am. J. Phys.* **66** 252

[Bar01]  Baranger M, de Aguiar M A M, Keck F, Korsch H J and Schellhaaß B 2001 *J. Phys. A: Math. Gen.* **34** 7227
[Ber89]  Berry M V 1989 *Proc. R. Soc.* A **422** 7
[Gar00]  Garashuk S and Tannor D J 2000 *Annu. Rev. Phys. Chem.* **51** 553
[Hel75]  Heller E J 1975 *J. Chem. Phys.* **62** 1544
[Hel87]  Huber D and Heller E J 1987 *J. Chem. Phys.* **87** 5302
[Hel88]  Huber D, Heller E J and Littlejohn R G 1988 *J. Chem. Phys.* **89** 2003
[Hel91]  Heller E J 1991 *J. Chem. Phys.* **94** 2723
[Hel02]  Van Voorhis T and Heller E J 2002 *Phys. Rev.* A **66** 50501
[Hel03]  Van Voorhis T and Heller E J 2003 *J. Chem. Phys.* **119** 12153
[Her84]  Herman M F and Kluk E 1984 *Chem. Phys.* **91** 27
[Kay94a]  Kay K G 1994 *J. Chem. Phys.* **100** 4377
[Kay94b]  Kay K G 1994 *J. Chem. Phys.* **100** 4432
[Kla85]  Klauder J R and Skagerstam B S 1985 *Coherent States, Applications in Physics and Mathematical Physics* (Singapore: World Scientific)
[Kla87]  Klauder J R 1987 Random media *The IMA Volume in Mathematics and its Applications* vol 7 ed G Papanicolau (New York: Springer) pp 163–82
[Mill70]  Miller W H 1970 *J. Chem. Phys.* **53** 3578
[Mill74]  Miller W H 1974 *Adv. Chem. Phys.* **25** 69
[Noi03]  Noid W G, Ezra G S and Loring R F 2003 *J. Chem. Phys.* **119** 1003
[Oni01]  Onishi T, Shudo A, Ikeda K S and Takahashi K 2001 *Phys. Rev.* E **64** 25201(R)
[Pol03]  Pollak E and Shao J 2003 *J. Phys. Chem.* A **107** 7112
[Rib04]  Ribeiro A D, de Aguiar M A M and Baranger M 2004 *Phys. Rev.* E **69** 66204
[Rub95]  Rubin A and Klauder J R 1995 *Ann. Phys. NY* **241** 212
[Shu95]  Shudo A and Ikeda K S 1995 *Phys. Rev. Lett.* **74** 682
[Shu96]  Shudo A and Ikeda K S 1996 *Phys. Rev. Lett.* **76** 4151
[Tan98]  Tanaka A 1998 *Phys. Rev. Lett.* **80** 1414
[Tho04]  Thoss M and Wang Haobin 2004 *Ann. Rev. Phys. Chem.* **55** 299
[Wan01]  Wang H, Thoss M, Sorge K, Gelabert R, Gimenez X and Miller W H 2001 *J. Chem. Phys.* **114** 2562
[Zha03]  Zhang S and Pollak E 2003 *Phys. Rev. Lett.* **91** 190201